water

MDPI

Article

Transient Flow Dynamics in Tesla Valve Configurations: Insights from Computational Fluid Dynamics Simulations

Mohamad Zeidan [1,*], Márton Németh [2], Gopinathan R. Abhijith [3], Richárd Wéber [2] and Avi Ostfeld [4]

1 KWR Water Research Institute, Groningenhaven 7, 3433 PE Nieuwegein, The Netherlands
2 Department of Hydrodynamic Systems, Budapest University of Technology and Economics, H-1111 Budapest, Hungary; mnemeth@hds.bme.hu (M.N.); rweber@hds.bme.hu (R.W.)
3 Department of Civil Engineering, BITS Pilani Hyderabad Campus, Hyderabad 500078, Telangana, India; abhi-jith.gr@hyderabad.bits-pilani.ac.in
4 Faculty of Civil and Environmental Engineering, Technion—Israel Institute of Technology, Haifa 32000, Israel; ostfeld@technion.ac.il
* Correspondence: mohamad.zeidan@kwrwater.nl

Abstract: This study investigates the transient flow dynamics and pressure interactions within Tesla valve configurations through comprehensive CFD simulations. Tesla valves offer efficient passive fluid control without the need for external power, making them favorable in various applications. Previous observations indicated that Tesla valves effectively reduce the amplitude of pressure transients, prolonging their duration and distributing energy over an extended timeframe. While suggesting a potential role for Tesla valves as pressure dampers during transient events, the specific mechanisms behind this behavior remain unexplored. This research focuses on elucidating the internal dynamics of Tesla valves during transient events, aiming to unravel the processes responsible for the observed attenuation in pressure transients. This study reveals the emergence of "pressure pockets" within Tesla valves, deviating from conventional uniform pressure fronts. These pockets manifest as discrete chambers with varying lengths and volumes, contributing to the non-uniform propagation of pressure throughout the system. This investigation employs advanced CFD simulations as a crucial tool to unravel the governing dynamics of transient flow within Tesla valve configurations. By elucidating underlying fluid dynamics, this study lays the groundwork for future Tesla valve design optimization, holding potential implications for applications where the control of transient flow events is crucial.

Keywords: transient flow; Tesla valve; CFD; protection device

Citation: Zeidan, M.; Németh, M.; Abhijith, G.R.; Wéber, R.; Ostfeld, A. Transient Flow Dynamics in Tesla Valve Configurations: Insights from Computational Fluid Dynamics Simulations. *Water* **2024**, *16*, 3492. https://doi.org/10.3390/w16233492

Academic Editor: Silvia Di Francesco

Received: 1 November 2024
Revised: 27 November 2024
Accepted: 2 December 2024
Published: 4 December 2024

1. Introduction

Surge protection in water distribution systems (WDSs) has been a longstanding concern, prompting the exploration of innovative passive check valves as alternatives to traditional protection devices. Among these, the Tesla valve has emerged as a promising solution, offering a fixed geometry design devoid of moving parts.

The concept of the Tesla valve, devised by Nikola Tesla in 1920, aimed to address the need for a valve that permits fluid flow in one direction while restricting it in the opposite direction—a fundamental requirement in mechanical applications where fluid impulses are directed accordingly. Although the notion of such fluid movements had been contemplated earlier in the design of valve components, prior implementations failed to fully capitalize on the concept's potential. Earlier valves relied on moving parts to control fluid impulses, rendering them prone to wear, intricate in design, expensive to manufacture, and inadequate for handling impulses effectively. Tesla introduced a unique channel through valvular action within the valve, thereby creating a No-Moving-Parts (NMP) valve, as highlighted by Zhang et al. [1], capable of meeting the desired

operational requirements. NMP valves offer reliability owing to their lack of apparent abrasion compared to conventional valves comprising moving parts.

Compared to the moving parts in traditional valves, the fixed geometry of Tesla valves addresses concerns related to wear, fatigue, and maintenance. This inherent design (Figure 1) has prompted investigations into the viability of Tesla valves as surge protection devices.

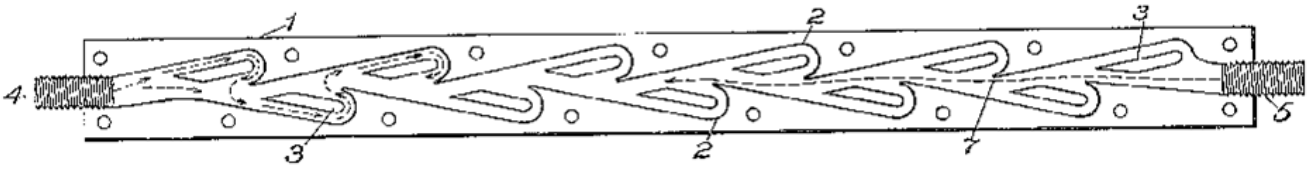

Figure 1. The cross-section of a Tesla valve, displaying its cavity design, from the original patent application (link).

In Figure 1, the forward direction is from right to left. The intricate design of the channels ensures that fluid can only travel in one direction, facilitating unobstructed flow while impeding flow in the opposite direction through geometric constraints. As a result, fluid within the Tesla valve follows a zigzag trajectory, encountering minimal resistance in the forward direction.

The Tesla valve functions as a fluid channel designed to modulate flow resistance based on the direction of fluid motion. It comprises a series of loops that interact with the passing fluid. The channel geometry is precisely engineered to enable unimpeded flow in one direction while imposing significant resistance or deceleration when flow occurs in the opposite direction. Unlike conventional valves, the Tesla valve achieves this flow modulation without needing mechanical moving parts [2].

1.1. Traditional Surge Protection Devices

In water distribution systems, pressure transient events represent critical phenomena that can significantly impact system performance and integrity. These transient events, characterized by rapid and often unpredictable changes in pressure, arise from various factors such as pump starts and stops, valve operations, and sudden changes in demand or flow rates [3]. These fluctuations in pressure can propagate throughout the distribution network, leading to a range of adverse effects, including pipe bursts, water hammer effects, and potential damage to infrastructure and equipment. The primary strategy for mitigating transient pressure amplitudes is to reduce the rate of change in velocity, effectively decreasing the amplitude of transient pressure. This understanding is supported by notable works in the field, including those by Tullis [4], Streeter and Wylie [5], and Thorley [6]. Various devices have been developed to safeguard water distribution systems from pressure surges [4,7]. These devices can be categorized into two distinct groups: those that directly affect the rate of change in velocity, such as surge vessels, flywheels, and surge towers, and those activated under specific conditions, including bypass check valves, pressure relief valves, air and vacuum valves, and feed tanks [8]. Devices in the former category exert an immediate and broad influence on system behavior, promptly impacting the system response. Conversely, pressure-limiting devices generally have a more localized impact. Additionally, the utilization of HDPE and similar viscoelastic material pipes has proven effective in dampening pressure waves [9]. Protection devices are commonly utilized in water distribution systems to act as mechanical barriers, absorbing energy and softening the impact of pressure transients. Despite their effectiveness in principle, these devices pose inherent challenges. The moving parts within them are prone to wear and fatigue, resulting in increased maintenance requirements. On the other hand, active surge protection methods, such as the utilization of pumps, air chambers, and relief valves, provide dynamic control over pressure variations. However, these systems necessitate substantial energy inputs,

intricate control mechanisms, and ongoing maintenance efforts. In the pursuit of more sustainable and cost-effective surge protection solutions, there has been a shift towards exploring passive check valves, with the Tesla valve emerging as a promising candidate.

1.2. Tesla Valve Applications

Previous research on Tesla valves has primarily focused on optimizing their design for various applications. For instance, Niu et al. [10] developed an apple pluck port based on negative pressure suction force inspired by the Tesla valve, enabling contactless apple plucking and reducing potential damage to the fruit. Similarly, Zhi-Jiang Jin et al. [11] proposed the use of Tesla valves to overcome seal issues in piping systems and achieve the decompression of hydrogen flow into fuel cells. Tesla valves are well suited for this purpose due to their design as check valves without moving parts, allowing for a significant pressure drop between the inlet and outlet during reverse flow. Additionally, Du et al. [12] introduced a Tesla-shaped drip emitter inspired by the structure of the Tesla valve. This emitter is designed to ensure effective energy dissipation, resulting in stable and uniform water flow to the soil layer. In their study, Liosis et al. [13] employed the Tesla valve as a micromixer to facilitate effective mixing between contaminated water and nanoparticles for the removal of heavy metals. Many more studies utilizing Tesla valves for micromixing can be found in the literature [14,15].

Our preliminary study [16] has indicated the potential of Tesla valves as low-cost alternatives to traditional surge protection methods. For instance, mounting a Tesla valve downstream of pumps has been proposed to reduce shock waves generated during pump shutdowns, replacing conventional protection devices. One of the notable advantages of Tesla valves is their scalability and adaptability to different dimensions and configurations. Studies have demonstrated the successful application of Tesla valves in various diameters, showcasing their potential in managing different tasks [10,17]. While previous studies have hinted at the promising attributes of Tesla valves in energy dissipation, there is a notable gap in understanding the detailed transient flow dynamics within Tesla valve configurations. This study aims to address this gap by employing advanced CFD simulations, offering a comprehensive exploration of the pressure interactions, flow patterns, and unique behaviors of Tesla valves during transient events.

2. Materials and Methods

The underlying principle of the Tesla valve as a surge protection device lies in the interference of waves inside the valve, leading to a damping effect without the need for moving parts or flow obstruction. This "soft" approach effectively prevents the propagation of pressure waves and safeguards the upstream section of the valve. Furthermore, the Tesla valve's geometry can be adjusted and modified to achieve the desired performance. It is vital to strike a balance between its performance during normal flow conditions and transient flow events, as an excessively efficient pressure protection device in transients may dissipate excessive energy during regular flow. Additionally, exploring different configurations of Tesla valves can offer alternative solutions. For instance, connecting Tesla valves in series increases damping capabilities but results in energy loss. Conversely, connecting them in parallel saves space and creates a more compact arrangement. A 3D configuration that combines both parallel and series connections can also be considered for optimal performance. In this study, the Tesla valve was employed and compared to a conventional pipeline for its ability to handle transient wave pressure surges (Figure 2). CFD models were created for both components, with varying dimensions, along with an increasing number of mesh parts for each dimension [18]. Accurate mesh modeling was crucial to ensure reliable results and prevent numerical instabilities.

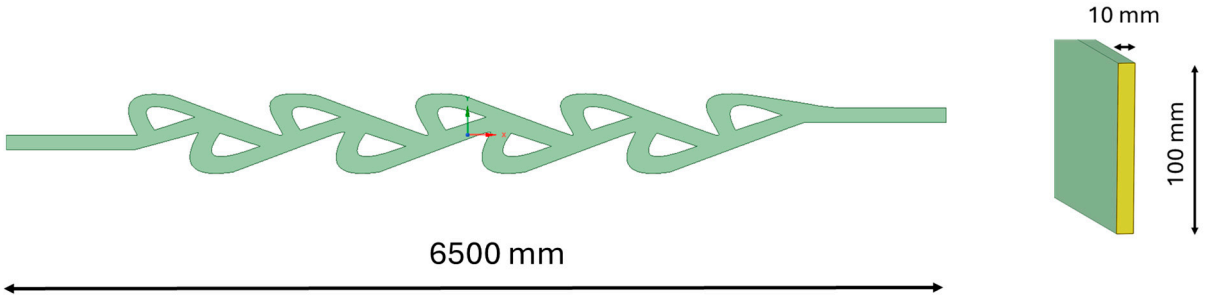

Figure 2. Tesla valve configuration for CFD modeling.

CFD Modeling Section

The geometry creations and fluid simulations were performed using the ANSYS 2023 R1 software and its modules. The geometry is based on a three-dimensional model that is freely available from grabcad.com. This geometry was cleaned, and all unnecessary parts were cut off using SpaceClaim to create the flow domain. It was scaled to have a height of 100 mm at the straight pipe section, and its width was set to contain only one cell to generate geometry for the two-dimensional simulations, as seen in Figure 3.

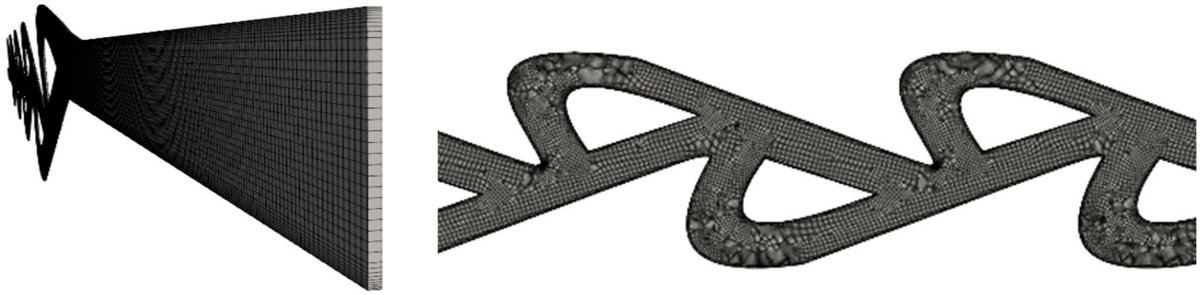

Figure 3. Two-dimensional mesh configuration (**left**); reference mesh of Tesla valve (**right**).

Mesh independence analysis is a crucial first step in CFD analysis to define a mesh, where the results of the simulations are independent of the mesh resolution [19,20]. A mesh independency analysis was performed by running transient simulations in the Tesla valve geometry with mesh sizes from 48,000 cells to 410,000 cells and calculating the maximum peak pressure and the time it takes to reach 10% of the peak pressure. Based on the independence analysis, the reference mesh size for the Tesla valve was chosen to be 150,000 cells (Figure 3). This mesh was generated by setting the target size of the hexahedral cells to be 0.004 mm, and the first element height of the inflation layer at the wall was set at 0.0004 mm, with a growth rate 1.2. This resulted in a y+ value of approximately 23, calculated with a reference velocity of 1 m/s. These mesh options resulted in mesh sizes that are given in Table 1.

Table 1. Approximate cell numbers of analyzed geometries.

Geometry Setup	Pipe (Short)	Tesla Valve	Pipe (Long)	Tesla Valve with Pipes
Geometry length (m)	6.5	6.5	26.5	26.5
Nr. of nodes	135,240	289,760	550,200	714,596
Nr. of elements	65,969	141,643	268,509	348,977
Volume (m^3)	0.0026	0.0058	0.0106	0.0138
Area (m^2)	1.35	2.98	5.51	7.15
Minimum element quality	0.1809	0.1805	0.0195	0.0195
Average element quality	0.7174	0.7172	0.7189	0.7186

It is important to note that this study did not employ a specific transient flow model. Instead, the transient behavior observed in the results was directly derived from the numerical solution of the governing equations. The ANSYS CFX module was used to calculate the Navier–Stokes equation for the fluid simulation. Compressible fluid was achieved by setting a function between pressure and density, as given below in Equation (1) [21]:

$$\rho = \rho_0 \left(1 + \frac{p}{B}\right), \quad (1)$$

where ρ_0 is the reference density of water, p is pressure, and B is the Bulk modulus, equal to 2.1 GPa.

The symmetricity boundary condition was set on the sides of the geometry to achieve a 2-dimensional simulation [22]. Further boundary conditions were set as constant velocity at the outlet and opening at the inlet with a constant pressure of 5 bar to allow for inflow and outflow. Finally, the wall roughness was set to 0.1 mm to account for relatively high friction inside the pipe or Tesla valve. In the transient simulations, an upwinding advection scheme and a second-order backward Euler transient scheme were used. The time step was set to 0.1 ms to focus on the immediate effect of the sudden closure of a valve downstream of the Tesla valve. The dynamic effect of a downstream valve closure was simulated by first running a steady-state simulation with a constant 1 m/s velocity at the outlet. The results of this steady-state simulation were used as the initial state of the following transient simulation, where the outlet velocity was reduced to either 0.8 m/s or 0.2 m/s. The pressure and velocity results were visualized and plotted using the free software Paraview 5.9.0.

3. Computational Results

The results obtained from CFD model simulations demonstrate the effectiveness of the Tesla valve in mitigating transient wave pressure surges compared to the conventional pipeline. To evaluate the performance of the Tesla valve in managing transient pressures, pressure plots over time were obtained at the upstream and downstream locations of both the Tesla valve and the conventional pipeline (see Figure 4). The pressure plot graph illustrates a damping effect in the Tesla valve case compared to the conventional pipeline. The simulations were conducted for a 5 s duration, with constant pressure at the inlet and constant velocity at the outlet. To assess the pressure-dissipating qualities of the Tesla valve, a pressure wave was generated by instantly changing the inlet velocity from 1.0 m/s to 0.8 m/s. A comparison was made between the Tesla valve results and those obtained from a straight pipe setup. This study also investigated the effect of geometry scaling by conducting simulations with three different diameters: 100 mm, 200 mm, and 300 mm. It was observed that pressure wave dissipation was slower in larger geometries. Although the Tesla valve reduced pressure wave amplitudes compared to the pipe case, it also increased the time required for dissipation. This difference between the Tesla valve and the pipe setup was more pronounced in larger geometries.

To understand the baseline behavior of Tesla valves, Figure 5 illustrates the normal flow in a Tesla valve, showcasing fluid movement in both the backward and forward directions. The fixed geometry of the Tesla valve creates a preferential direction of flow, allowing fluid to traverse with minimal resistance in one direction and acting as a nearly impenetrable barrier in the opposite direction. This inherent design is essential for comprehending the subsequent analyses of transient events within the Tesla valve.

Figure 6 presents detailed transient wave simulations for Tesla valves and a conventional pipe for diameters of 100 mm, 200 mm, and 300 mm. These simulations aim to showcase the capability of Tesla valves in reducing wave amplitudes and extending their duration during transient flow events. The results provide crucial insights into how the geometry of Tesla valves influences the transient behavior of fluid within the system.

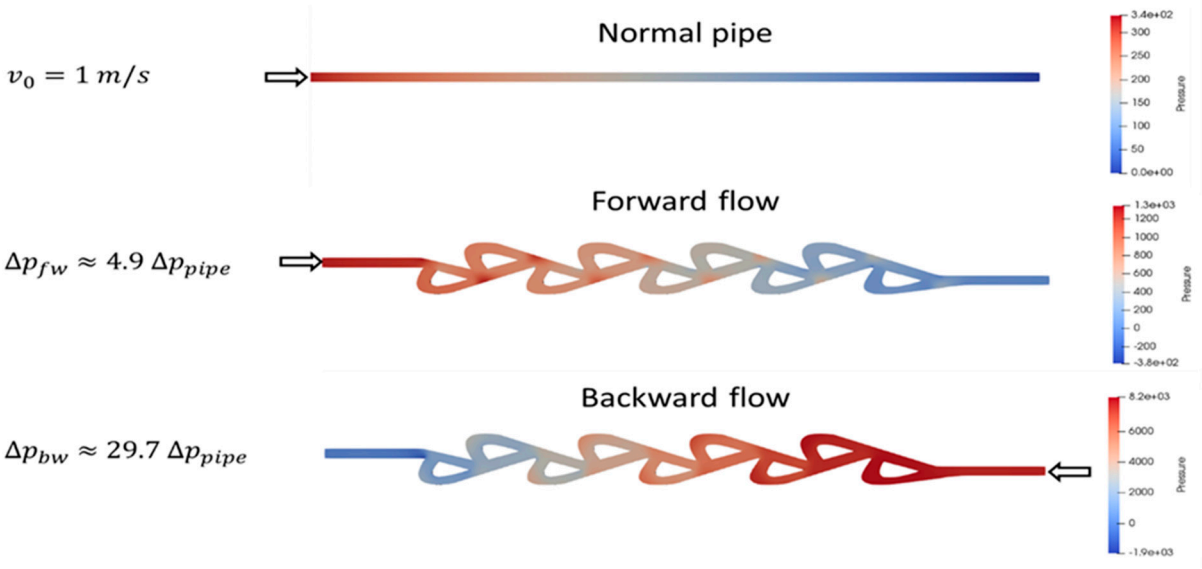

Figure 4. Normal pressure characteristics in Tesla valve.

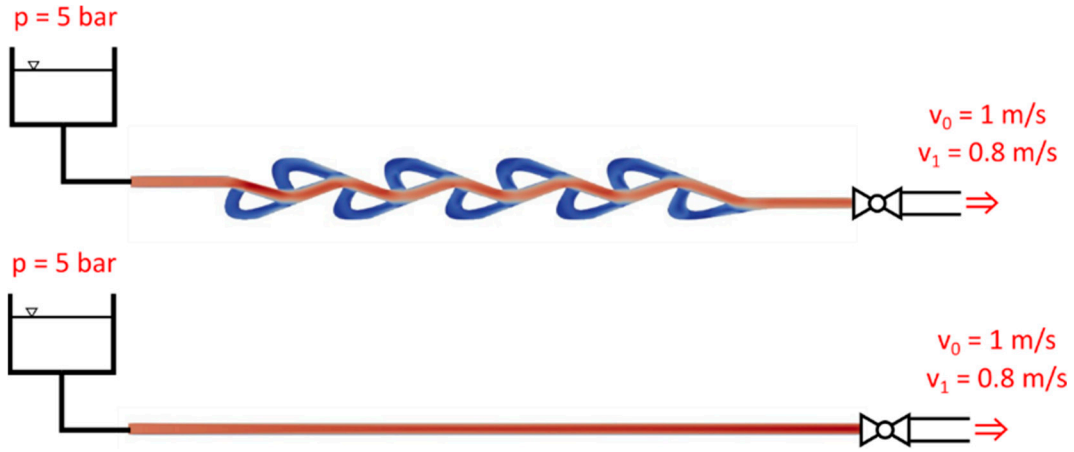

Figure 5. Network layout for simulating transient flow in normal pipe (**above**) vs. Tesla valve (**bottom**). Color map depicts velocity values.

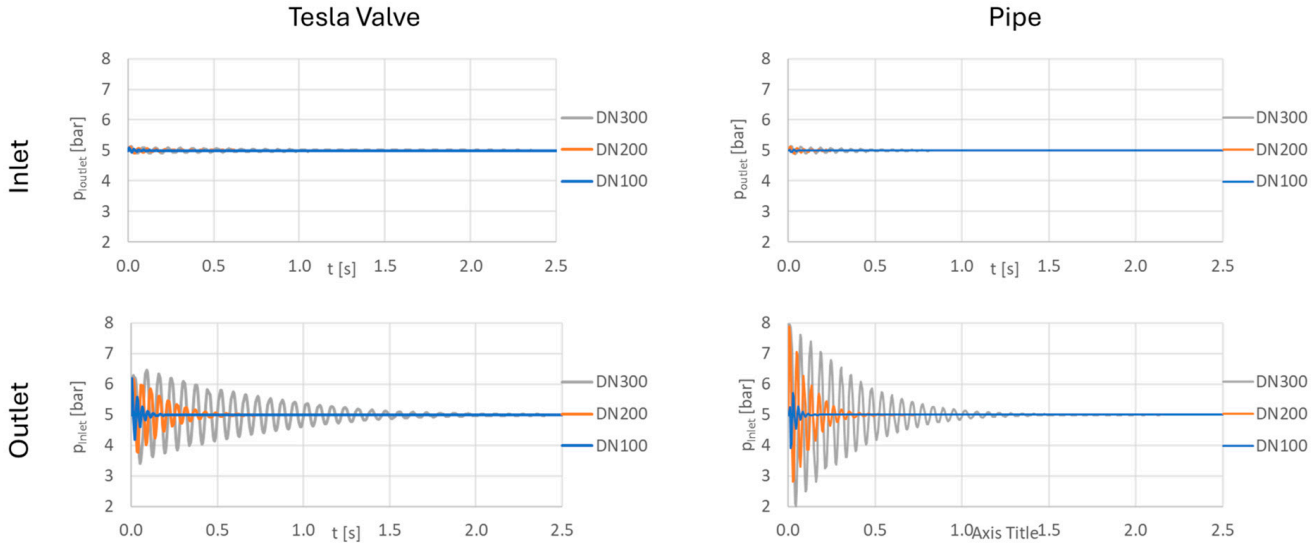

Figure 6. The transient response for the Tesla valve and pipe system for 3 different diameters.

In Figure 7, we compare the normalized absolute pressure for both the conventional pipeline and Tesla valve cases. This analysis provides a quantitative understanding of pressure variations in different configurations. Examining the normalized pressure allows for a direct comparison, highlighting the efficiency of Tesla valves in managing transient pressures.

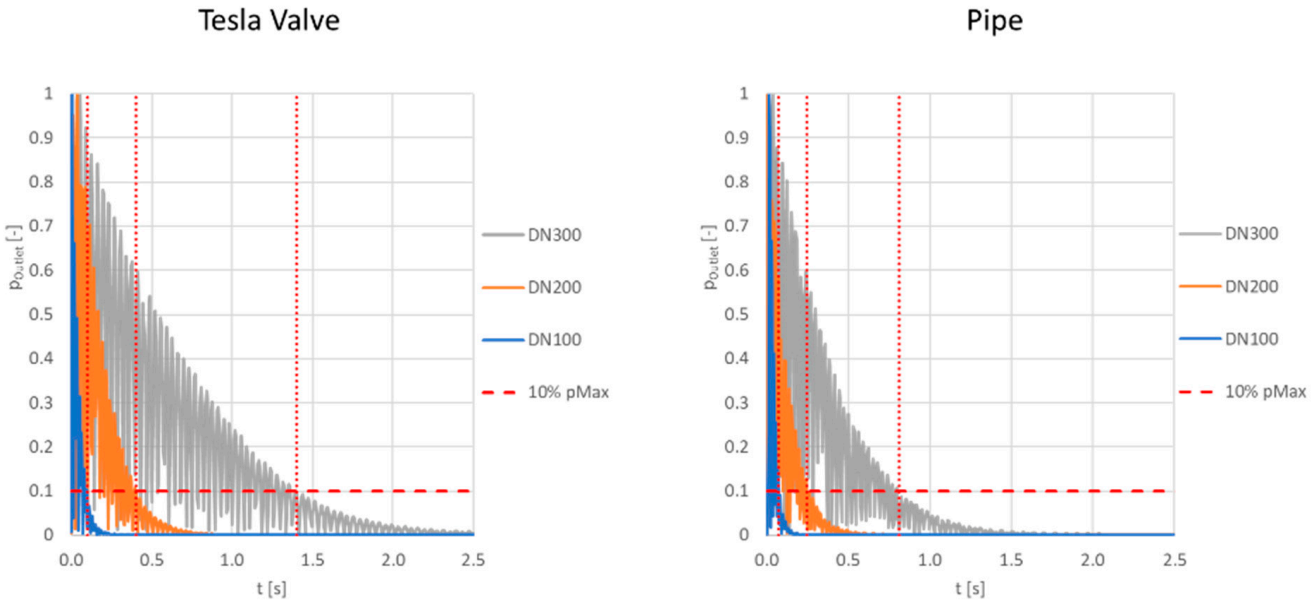

Figure 7. The normalized pressure response for the Tesla valve and pipe systems.

Figure 8 depicts the transient response (pressure over time) for Tesla valves versus normal pipes in a 5 s simulation. This temporal analysis aims to reveal the dynamics of pressure fluctuations during transient events and how Tesla valves effectively mitigate the impact over time.

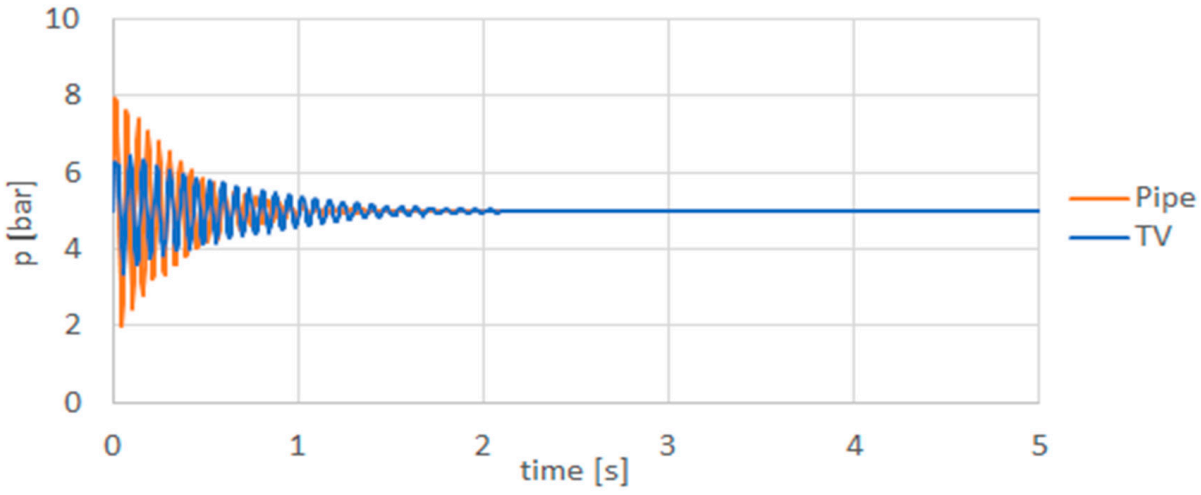

Figure 8. The transient response for the Tesla valve vs. pipes for 5 s.

Figure 9 focuses on the distinctive phenomenon of pressure pockets within the Tesla valve during transient events. Sub-figures at different time steps illustrate the evolution and presence of pressure pockets. These pockets contribute to the prolonged duration of transient pressure events and are crucial in understanding the unique behavior of Tesla valves. From Figure 8, we can see that the pressure inside the channel was significantly reduced after the convergence of the main flow and the secondary flow. This further

indicated that hedging the two water flows could produce relatively large head loss and achieve a good energy dissipation effect.

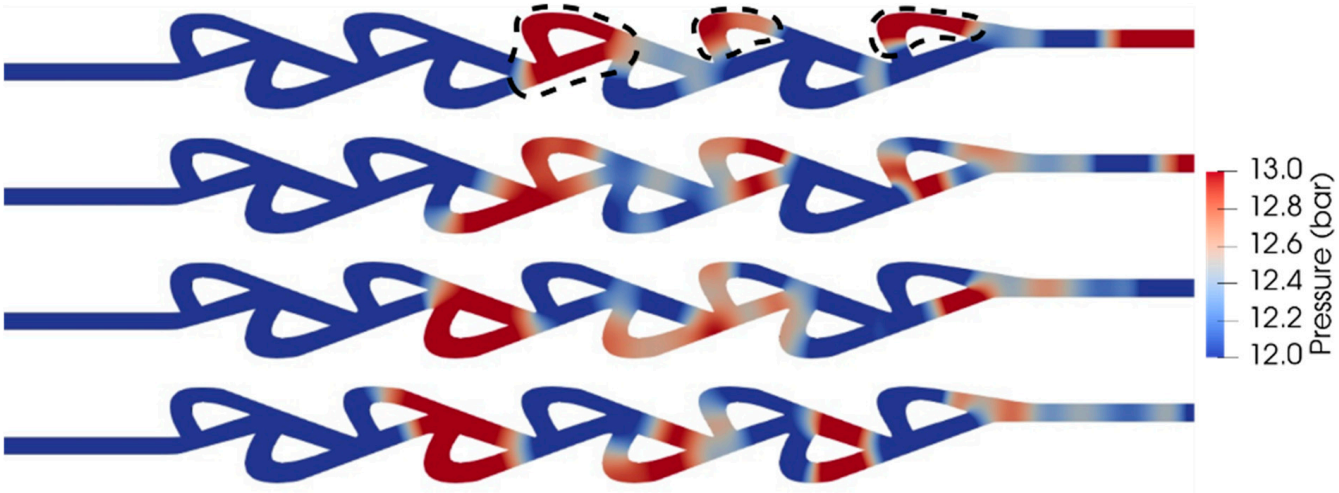

Figure 9. Pressure pockets highlighted in the CFD simulation at different time steps.

Figure 10 aims to illustrate potential scenarios of pressure pockets within the Tesla valve, highlighting the interactions between high-pressure fronts and low-pressure zones, as well as the assumed exerted force vectors. This visualization aligns with the hypothesis underlying the ability of the Tesla valve to mitigate pressure transients. By depicting the spatial distribution of pressure variations and the corresponding force vectors, Figure 9 provides valuable insights into the dynamic behavior of fluid flow within the Tesla valve configuration. Through this visualization, we seek to elucidate the mechanisms through which the Tesla valve effectively attenuates pressure transients, contributing to a deeper understanding of its functionality and potential applications in fluid control systems.

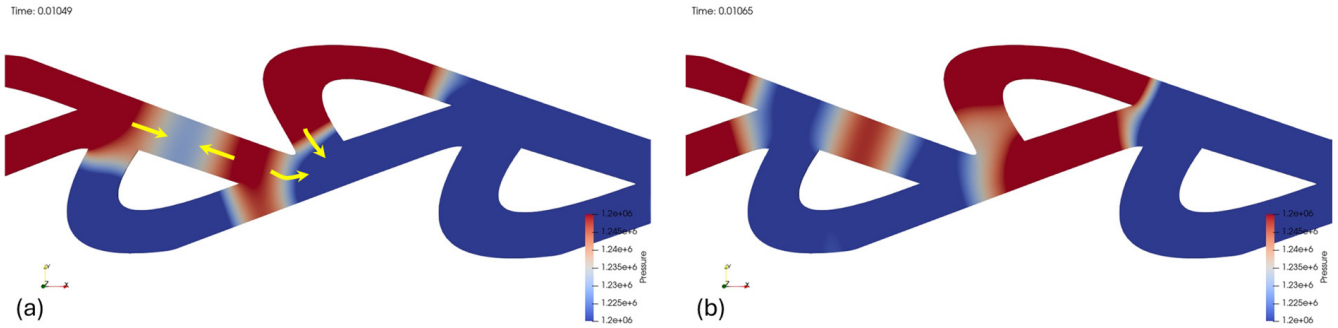

Figure 10. The projected trajectory for the pressure fronts from high to low pressure. (**a**) illustrate the pressure pockets at 0.01049 s, while (**b**) shows the pressures a 0.16 millisecond after.

To quantitatively characterize the pressure pocket phenomena, pressure and velocity measurements were conducted at seven specific points within the third lower chamber of the Tesla valve. The locations of these measurement points are illustrated in Figure 11, providing a comprehensive spatial reference for the data collection process. By systematically capturing pressure and velocity data at these defined points, we aim to gain insights into the distribution and dynamics of pressure pockets within the Tesla valve configuration.

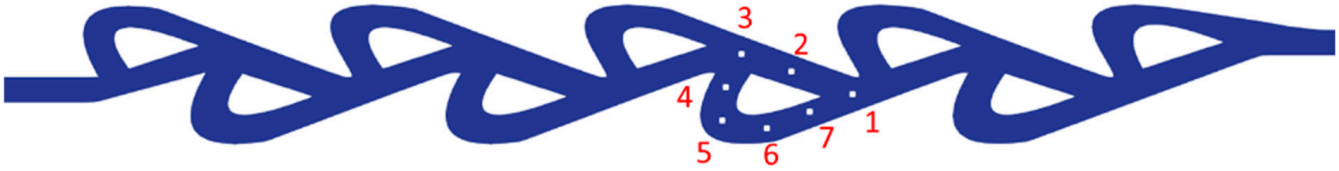

Figure 11. Measurement points in the third lower chamber of the Tesla valve. The numbering (1–7) indicates specific locations used in the CFD simulation to extract detailed flow and pressure data for analysis.

Figures A1 and A2 illustrate the measured pressures and velocities at the seven points over 5 s, with a time step of 10 μs. To illustrate the non-uniform propagation of pressure fronts within the Tesla valve, pressure readings at points 1, 3, and 5 are analyzed. These points were selected as they represent the behavior at the corners of the chamber. Figure 12 presents the pressure plots, with dashed lines indicating the timestamps corresponding to the accompanying snapshots.

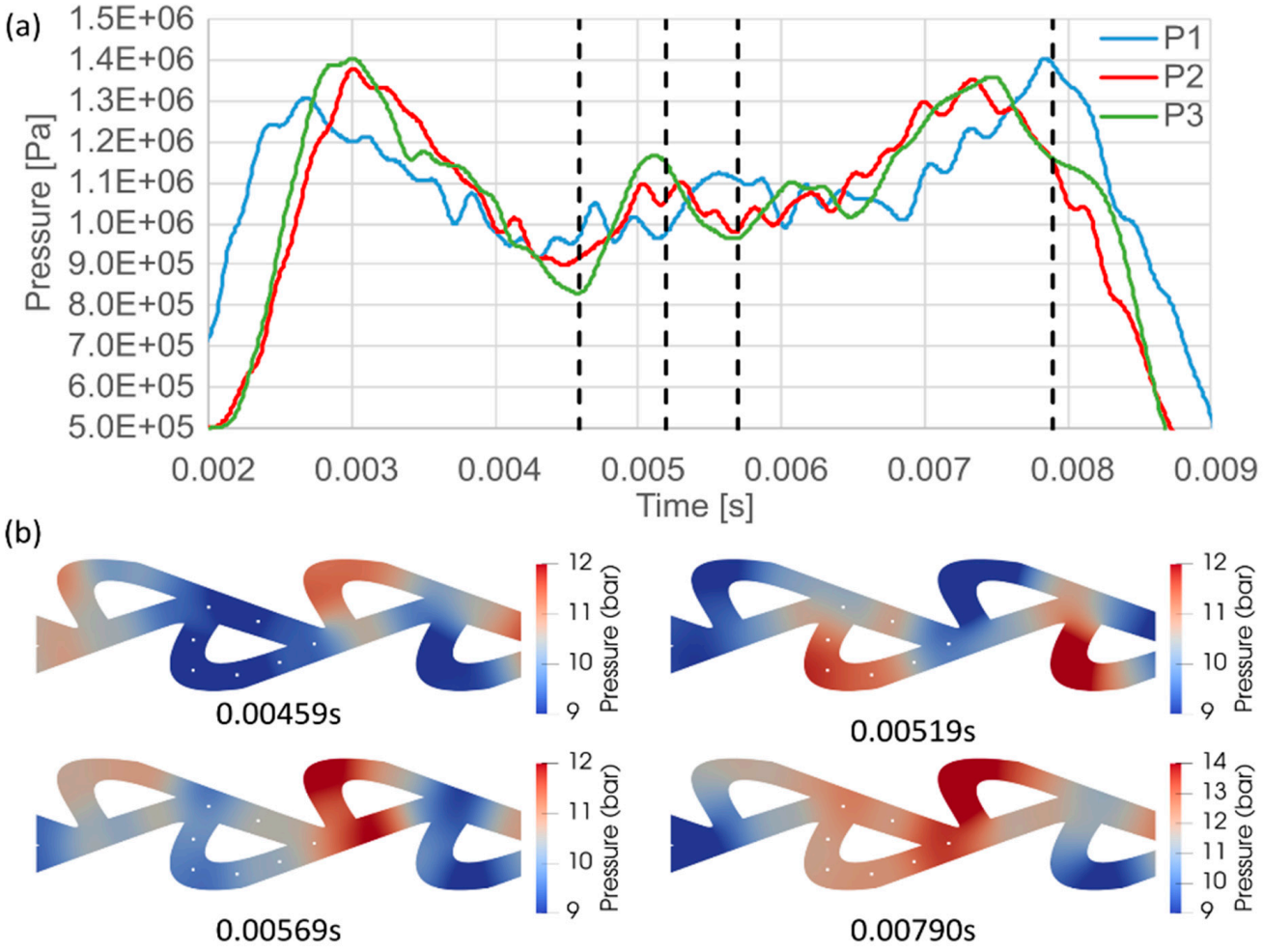

Figure 12. (**a**) Pressure readings at points 1, 3, and 5. Dashed lines indicate timestamps corresponding to accompanying snapshots at different timestamps shown in (**b**).

The pressure plot in Figure 12a reveals noticeable variations in both time and amplitude. Despite the lack of distinct compartmentalization within the chambers, differences between them are evident. Specifically, the snapshots [Figure 12b] depict instances where low-pressure chambers occur between two high-pressure chambers. A finer time scale is imperative for a more comprehensive understanding of the interaction among pressure

pockets within the chambers. Figure 13 displays pressure plots within the interval of 0.010 to 0.020 s, facilitating a detailed examination of the dynamics during this crucial timeframe.

As seen in Figure 13, the pressure amplitudes at points 1 and 6 exhibit a temporal phase shift. This temporal misalignment manifests that the peak pressure amplitude at point 1 coincides with the nadir of pressure at point 6. Conversely, the peak pressure amplitude at point 6 aligns with the nadir of pressure at point 1. This phase shift indicates a temporal disparity in the oscillatory behavior of pressure fluctuations between the two points. The pressure at point 7 falls intermediary to the extremities represented by the pressure amplitudes at points 1 and 6. The temporal phase shift observed between points 1 and 6 exerts dynamic forces that influence the flow dynamics at point 7. Notably, between the time interval of 0.017 to 0.018 s, this influence results in a discernible acceleration observed at point 7, as can be seen in Figure 14.

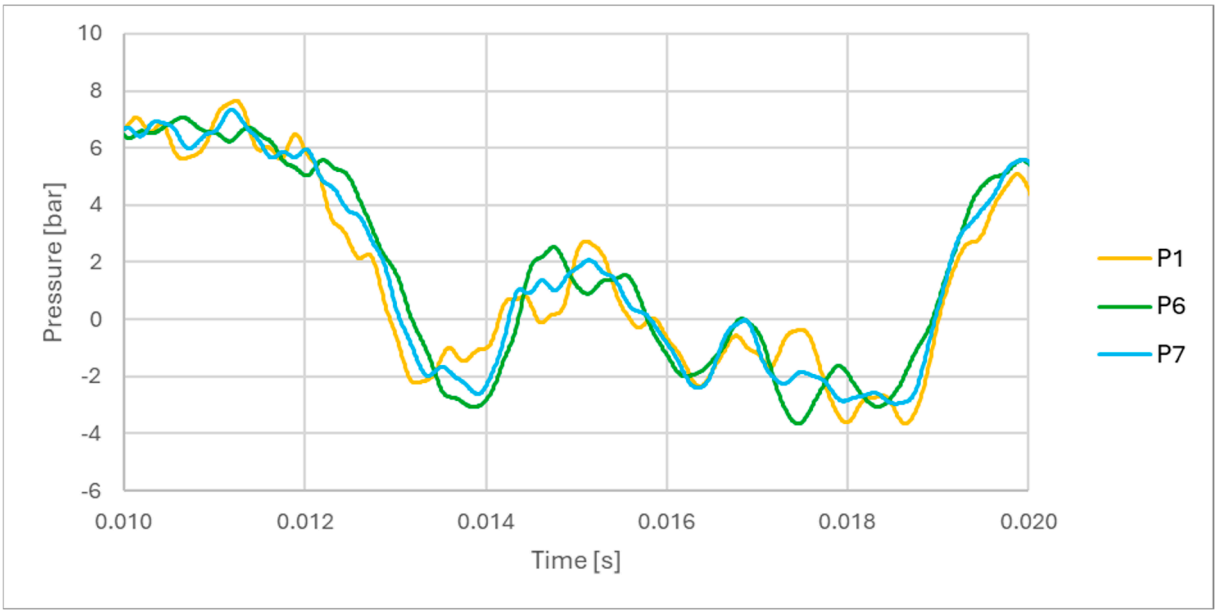

Figure 13. Pressure plot at points 1, 6, and 7.

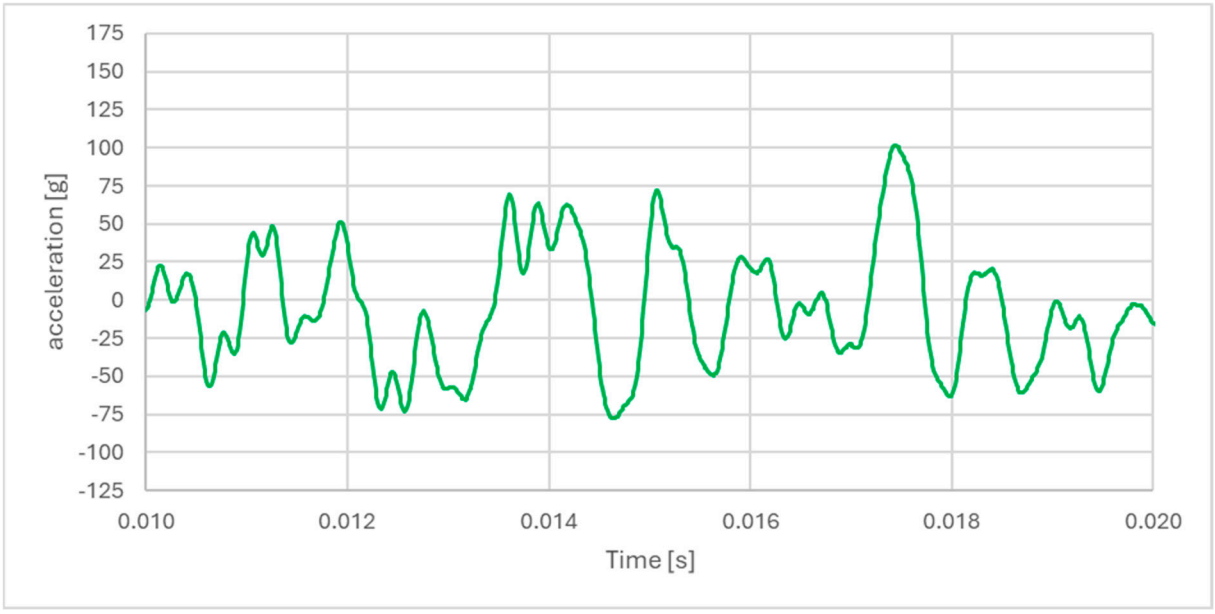

Figure 14. Acceleration at point 7.

Figure 15a presents the pressure differentials between points 2–1 and 2–3, while Figure 15b presents the resultant net pressure at point 2. The upper plot reveals a distinct asymmetry: when the pressure difference between points 2 and 1 is positive, the pressure difference between points 2 and 3 becomes negative and vice versa. This counteracting behavior leads to a reduction in the overall pressure gradient at point 2. This phenomenon underscores the impact of the Tesla valve's geometry on pressure wave propagation, where opposing pressure forces diminish each other, rather than creating a uniform pressure front.

Overall, our CFD simulations yielded valuable insights into the transient flow dynamics within Tesla valve configurations. The analysis discerned the emergence of distinct pressure pockets within the valve, both between different chambers and within the chambers themselves, significantly influencing the non-uniform propagation of pressure. Notably, our findings unveiled a temporal phase shift between pressure amplitudes at various points within the valve, highlighting dynamic interactions that substantially impact flow dynamics. These interactions play a crucial role in modulating the amplitude and duration of transient pressure events.

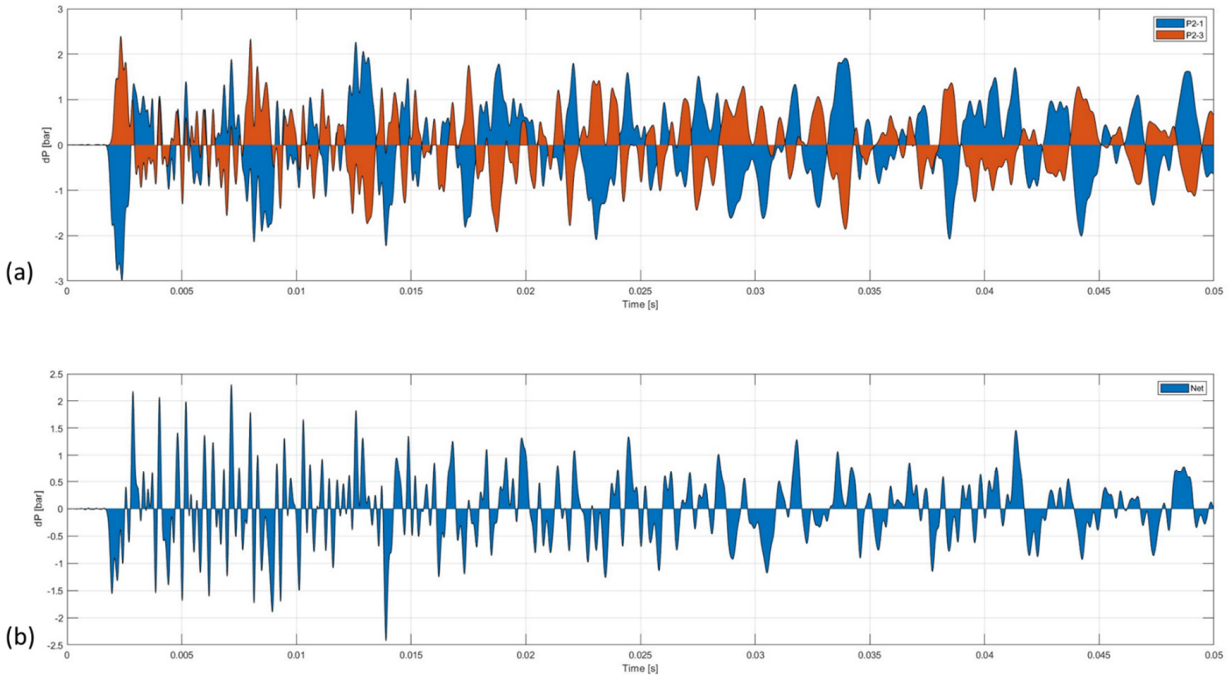

Figure 15. (**a**) Pressure fluctuations at points 1 and 3 variations over time. (**b**) The superposition of the two pressure signals, illustrating their combined effect and the resulting net pressure at point 2.

4. Conclusions

This study provided comprehensive insights into the transient flow dynamics of Tesla valve configurations, emphasizing their potential applications in water distribution systems. Through our simulations, we enhanced our understanding of the transient flow dynamics within Tesla valves, focusing on elucidating the interference of pressure waves within the valve and their influence on pressure wave propagation. This study demonstrated the efficacy of Tesla valves as transient protection devices in water distribution systems through CFD simulations. The results clearly depict the damping effect of Tesla valves, effectively reducing pressure wave amplitudes and highlighting their promising potential as a cost-effective solution for managing pressure transients in WDSs. Notably, our analysis revealed the emergence of distinct pressure pockets within the valve, both between different chambers and within the chambers themselves, significantly influencing the non-uniform propagation of pressure. Moreover, we observed a temporal phase shift between pressure amplitudes at various points within the valve, indicating dynamic interactions that substantially impact flow dynamics. These interactions play

a crucial role in modulating the amplitude and duration of transient pressure events. While our findings provide a foundational understanding of these mechanisms, further work is required to systematically analyze the influence of valve size and configuration on transient damping.

Despite the progress made in understanding the transient flow dynamics within Tesla valves, certain gaps in knowledge persist. A comprehensive understanding of the underlying fluid dynamics during transient events and the mechanisms responsible for the observed behavior is crucial for further advancements. The detailed exploration of pressure interactions, flow patterns, and unique behaviors within Tesla valves during transient events remains an ongoing area of research. The evolution of research in surge protection, particularly in the context of Tesla valves, represents a paradigm shift in the quest for sustainable and efficient solutions. As water distribution systems face increasing demands and challenges, the simplicity, scalability, and effectiveness of Tesla valves make them a compelling area of investigation. Future research directions may include experimental validations, real-world applications, and further optimizations of Tesla valve designs to fully exploit their potential in transient flow control within water distribution systems.

Author Contributions: Conceptualization, M.Z., M.N., R.W., G.R.A. and A.O.; methodology, M.Z., M.N. and R.W.; software, M.N. and R.W.; validation, M.Z., M.N., R.W. and A.O.; formal analysis, M.N. and R.W.; investigation, M.Z., M.N. and R.W.; resources, M.Z., M.N. and R.W.; data curation, M.Z.; writing—original draft preparation, M.Z.; writing—review and editing, M.Z., M.N., R.W., G.R.A. and A.O.; visualization, M.N. and R.W.; supervision, R.W. and A.O.; project administration, M.Z. and A.O.; funding acquisition, R.W. and A.O. All authors have read and agreed to the published version of the manuscript.

Funding: Project no. TKP-6-6/PALY-2021 was implemented with the support provided by the Ministry of Culture and Innovation of Hungary from the National Research, Development and Innovation Fund, financed under the TKP2021-NVA funding scheme. This research was also supported by The Bernard M. Gordon Center for Systems Engineering at the Technion.

Data Availability Statement: The data presented in this study are available on request from the corresponding author.

Acknowledgments: The authors thank the Ministry of Culture and Innovation of Hungary and The Bernard M. Gordon Center for Systems Engineering at the Technion for their support. They also acknowledge the valuable feedback provided by colleagues and reviewers during the study.

Conflicts of Interest: The authors declare no conflicts of interest.

Appendix A

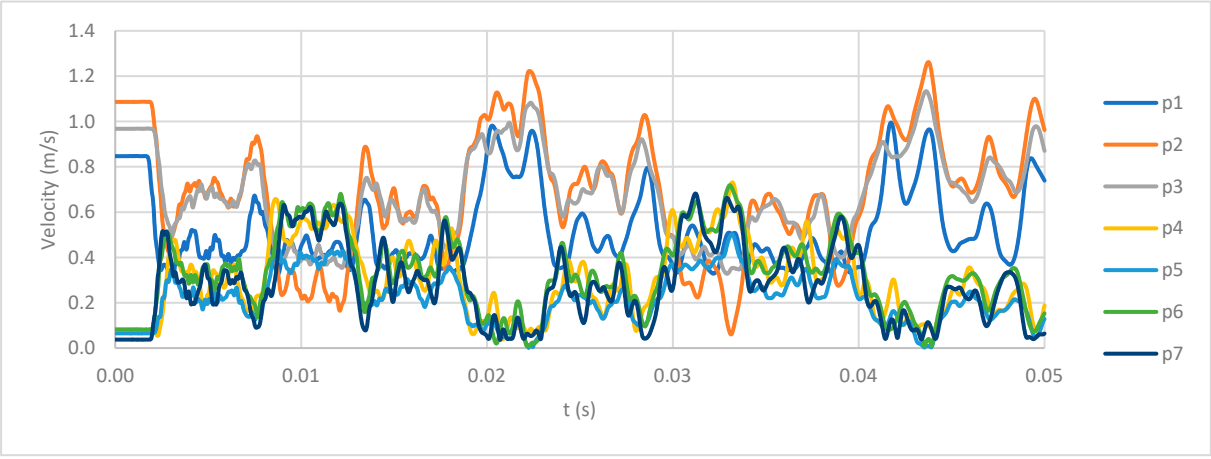

Figure A1. Velocity plots at the 7 measuring points over the simulation period.

Appendix B

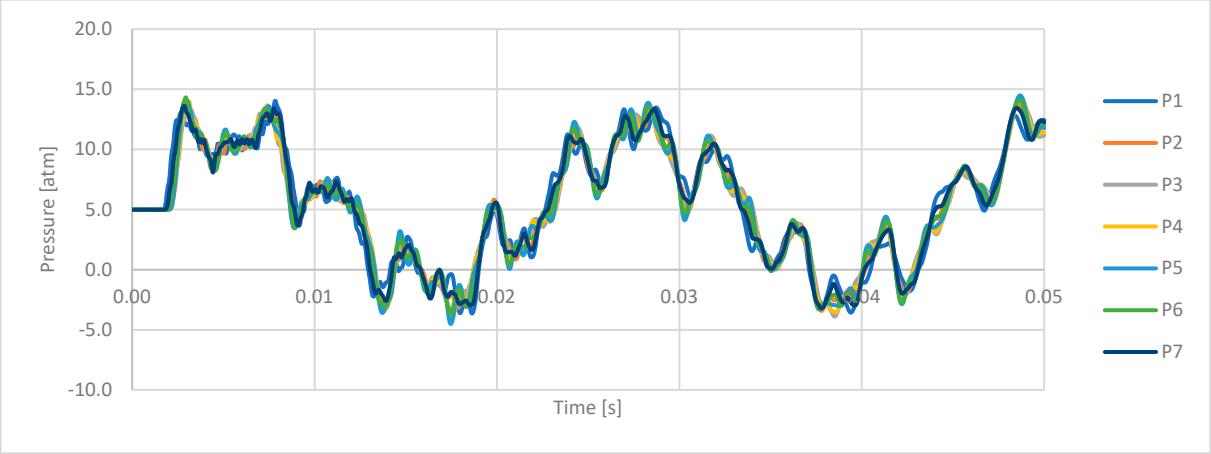

Figure A2. Pressure plots at the 7 measuring points over the simulation period.

References

1. Zhang, S.; Winoto, S.H.; Low, H.T. *Performance Simulations of Tesla Microfluidic*; MNC2007-21107; Department of Mechanical Engineering, National University of Singapore: Singapore, 2007.
2. Bäckman, E.; Willén, M. Tesla Valve for Hydrogen Decompression: Fluid Dynamic Analysis. Bachelor's Thesis, KTH Royal Institute of Technology, Stockholm, Sweden, 2019.
3. Ghidaoui, M.S.; Zhao, M.; McInnis, D.A.; Axworthy, D.H. A Review of Water Hammer Theory and Practice. *Appl. Mech. Rev.* **2005**, *58*, 49–76. [CrossRef]
4. Tullis, J.P. *Hydraulics of Pipelines, Pumps, Valves, Cavitation, Transients*; John Wiley & Sons: New York, NY, USA, 1989.
5. Streeter, V.L.; Wylie, E. *Fluid Transients in Systems*; Prentice-Hall: New York, NY, USA, 1993.
6. Thorley, A.R.D. *Fluid Transients in Pipeline Systems*; Professional Engineering Publishing Ltd.: London, UK, 2004.
7. Kim, S.-G.; Lee, K.-B.; Kim, K.-Y. Water hammer in the pump-rising pipeline system with an air chamber. *J. Hydrodyn.* **2014**, *26*, 960–964. [CrossRef]
8. Pothof, I.; Karney, B. Guidelines for transient analysis in water transmission and distribution systems. In *Water Supply System Analysis-Selected Topics*; IntechOpen: Rijeka, Croatia, 2012.
9. Evangelista, S.; Leopardi, A.; Pignatelli, R.; de Marinis, G. Hydraulic Transients in Viscoelastic Branched Pipelines. *J. Hydraul. Eng.* **2015**, *141*, 04015016. [CrossRef]
10. Niu, Z.; Xu, S.; Jiang, J.; Zhang, J. Design and Optimization of Strength type Negative Pressure Suction Force Pluck Port Based on Tesla Valve. 2021.
11. Jin, Z.-J.; Gao, Z.-X.; Chen, M.-R.; Qian, J.-Y. Parametric study on Tesla valve with reverse flow for hydrogen decompression. *Int. J. Hydrogen Energy* **2018**, *43*, 8888–8896. [CrossRef]
12. Du, P.; Li, Z.; Hao, R.; Ma, J.; Yan, D. Hydraulic Performance and Energy Dissipation Mechanism Analysis of the Tesla-Shaped Emitter. *Energies* **2023**, *16*, 5375. [CrossRef]
13. Liosis, C.; Sofiadis, G.; Karvelas, E.; Karakasidis, T.; Sarris, I. Simulations of Tesla Valve Micromixer for Water Purification with Fe_3O_4 Nanoparticles. *Environ. Sci. Proc.* **2022**, *21*, 82. [CrossRef]
14. Anagnostopoulos, J.S.; Mathioulakis, D.S. Numerical simulation and hydrodynamic design optimization of a tesla-type valve for micropumps. *IASME Trans.* **2005**, *2*, 1846–1852.
15. Wang, C.T.; Chen, Y.M.; Hong, P.A.; Wang, Y.T. Tesla valves in micromixers. *Int. J. Chem. React. Eng.* **2014**, *12*, 397–403. [CrossRef]
16. Zeidan, M.; Németh, M.; Wéber, R.; Ostfeld, A. Assessing the Efficacy of Tesla Valves as Transient Protection Devices in Water Distribution Systems. In Proceedings of the 19th International Computing and Control for Water Industry Conference, Leicester, UK, 4–7 September 2023.
17. Chandavar, R.A. Stability analysis of tesla valve based natural circulation loop for decay heat removal in nuclear power plants. In Proceedings of the 2019 Advances in Science and Engineering Technology International Conferences (ASET), Dubai, United Arab Emirates, 26 March–10 April 2019; pp. 1–6.
18. Anderson, J. *Computational Fluid Dynamics*; McGraw-Hill Series in Mechanical Engineering; McGraw-Hill: New York, NY, USA, 1995.
19. Katz, A.; Snakaran, V. Mesh quality effects on the accuracy of CFD solution on unstructured meshes. *J. Comput. Phys.* **2011**, *230*, 7670–7686. [CrossRef]
20. Alauzet, F.; Frey, P.J.; George, P.L.; Mohammadi, B. 3D transient fixed point mesh adaptation for time-dependent problems: Application to CFD simulation. *J. Comput. Phys* **2006**, *222*, 592–623. [CrossRef]

21. Wéber, R.; Hős, C. Experimental, Numerical Analysis of Hydraulic Transients in the Presence of Air Valve. *Period. Polytech. Mech. Eng.* **2018**, *62*, 1–9. [CrossRef]
22. Ceuca, S.C.; Macián-Juan, R. CFD simulation of direct contact condensation with ANSYS CFX using locally defined heat transfer coefficients. In Proceedings of the 20th International Conference on Nuclear Engineering, Anaheim, CA, USA, 30 July–3 August 2012. [CrossRef]